

Photonic stopbands and light transmission characteristics in GaAs-based three dimensional waveguides with large index contrast

Pallab Bhattacharya,^{a)} Weidong Zhou, Donghai Zhu, and Jayshri Sabarinathan

Department of Electrical Engineering and Computer Science, Solid State Electronics Laboratory,
University of Michigan, Ann Arbor, Michigan 48109-2122

(Received 19 March 1999; accepted for publication 23 July 1999)

A relatively simple technique to realize a III–V semiconductor based quasi-three-dimensional photonic crystal material with a refractive index contrast ~ 2 is described. Fourier transform infrared spectroscopy measurement reveals a stop band between 15 and 20 μm for a sample with scattering center spacing of 6.3 μm . Another narrow transmittance dip is observable in the wavelength range of 1.1–1.58 μm , with an attenuation of 12 dB at 1.18 μm . The relation between transmission T and waveguide length L , as measured by 1.15 μm wavelength light is either $T \sim L^{-2}$ or $T \sim \exp(-L/L_0)$, indicating photon localization in the weakly disordered system. © 1999 American Institute of Physics. [S0003-6951(99)03238-6]

Coherent multiple scattering of light in a disordered photonic medium can lead to light localization (a greatly reduced photon transport velocity) and the propagation of light in an ordered photonic crystal can lead to the formation of a photonic band gap (PBG) characterized by stop and pass bands.^{1–5} Such photonic gaps have been observed in two- and three-dimensional (3D) metallic, dielectric, and acoustic structures.^{6,7} Most of these structures are at the macroscopic level. Recently photonic gaps have been demonstrated in silicon and GaAs-based nanometer scale “woodpile” structures.^{8–10}

There are several seemingly insurmountable challenges: first and foremost, it would be desirable to realize the photonic crystal with III–V direct band gap semiconductors, such as GaAs, AlGaAs, InP, InGaAsP, etc., in which the radiative efficiency is high. It is also desirable to create 3D medium. Second, the refractive index contrast needs to be large, and the spacing of the dielectric scatterers should be of the order of λ/n in these materials,² or $kl \approx 1$, where λ is the vacuum wavelength, n is the effective refractive index of the material, l is the photon mean free path, and \mathbf{k} is the wave vector. Finally, for some applications, it may be desirable to delineate waveguides on which contacts, or electrodes, can be formed. Above all, the processing technique should be relatively simple and reproducible.

We report here a relatively simple technique to realize a III–V semiconductor based quasi-3D photonic crystal in which a single epitaxial growth, Zn diffusion, wet oxidation, and conventional processing steps are used. Due to the nature of the diffusion process, the nonuniformity of the scatterer size introduces a weak disorder³ in the crystal. We have fabricated waveguides with the photonic crystals and have made transmission and Fourier transform infrared spectroscopy (FTIR) measurements on these samples.

The photonic crystal is made with the heterostructure, shown in the inset of Fig. 1, grown by molecular beam epitaxy on a (001)-oriented GaAs substrate. After growing a 0.1 μm GaAs buffer layer, a 0.2 μm $\text{Al}_{0.98}\text{Ga}_{0.02}\text{As}$ etch stop

layer, and a 0.5 μm GaAs etch protection layer, the active region is grown. It consists of a 1 μm thick layer of $\text{Al}_{0.98}\text{Ga}_{0.02}\text{As}$ followed by six periods of 0.18 μm of $\text{Al}_{0.8}\text{Ga}_{0.2}\text{As}$ and a multiquantum well (MQW) region. The latter consists of 20 pairs of 20 Å GaAs and 150 Å $\text{Al}_{0.8}\text{Ga}_{0.2}\text{As}$ layers. The total thickness of the active region is 3.14 μm . A protective 200 Å GaAs cap layer is finally grown. The entire heterostructure is undoped.

A 0.1 μm thick layer of Si_xN_y is first deposited on the surface of the grown heterostructure and patterned into circular disks, to form a centered hexagonal pattern, by standard optical lithography. The center-to-center spacing a is 6.3 μm . The deep zinc diffusion step is carried out with a ZnAs_2 source in an evacuated quartz ampoule at 575 °C for 90 min. Impurity-induced layer disordering¹¹ takes place selectively in the MQW regions through the openings between the Si_xN_y disks and converts it into a uniform $\text{Al}_{0.78}\text{Ga}_{0.22}\text{As}$ alloy. Ridges of width 30 μm and length varying in the range of 600–1800 μm are formed by standard optical lithography and a combination of wet and dry etching. The sample is

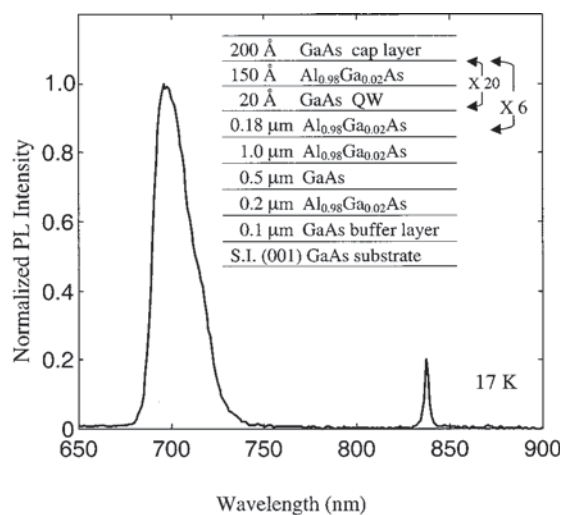


FIG. 1. Low temperature (17 K) photoluminescence spectrum of the GaAs-based heterostructure grown by molecular beam epitaxy (shown in the inset) and used to form the PBG material.

^{a)}Electronic mail: pkb@eecs.umich.edu

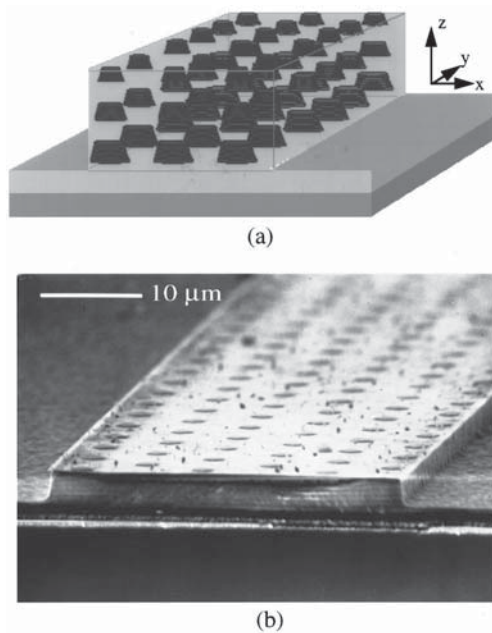


FIG. 2. (a) Schematic, and (b) SEM image of GaAs-based PBG waveguide made by Zn diffusion, wet oxidation, and etching techniques. The MQW scattering regions are faintly visible in the SEM image. Si_3N_4 disks (reduced in size during processing) are seen on the top surface.

then inserted in an open-tube quartz furnace and wet oxidation is performed at 450 °C for 15 h by flowing N_2 saturated with water vapor by bubbling it through a water bath held at 95 °C. Both epitaxially grown $\text{Al}_{0.98}\text{Ga}_{0.02}\text{As}$ and intermixed $\text{Al}_{0.78}\text{Ga}_{0.22}\text{As}$ regions are uniformly oxidized to form the insulator Al_xO_y .¹² It may be noted that under the hydrolysis conditions used, the thin 150 Å $\text{Al}_{0.8}\text{Ga}_{0.2}\text{As}$ layers within the nonintermixed MQW regions are not oxidized, because the oxidation rate¹³ is negligible for this thickness. We have now created a photonic crystal in which small MQW regions of average refractive index ~ 3.55 are embedded in an Al_xO_y medium of refractive index ~ 1.5 .¹⁴ The index contrast is therefore >2.0 . A disadvantage of this process is the considerable lateral diffusion of zinc during the deep diffusion step. It is estimated that the scattering center radius r varies in the range of 0.15–1.5 μm . The GaAs substrate is finally removed by selective wet etching and the waveguides are mounted on glass substrates. Similar processing steps have been used¹⁵ to form a 2D photonic lattice. The scanning electron microscope (SEM) image of the waveguide along with a schematic is shown in Fig. 2.

It is important to understand the nature of the fabricated crystal. If the diffusion was perfect (no lateral spreading), then the structure would be a set of centered hexagonal high-index rods, with periodic gaps, immersed in the low index Al_xO_y . However, because of the considerable lateral diffusion of Zn with depth, there is a variation in the size of MQW regions with depth. We therefore choose to describe our structure as a quasi-3D, or weakly disordered crystal. It may not have true 3D photonic band gaps but should demonstrate stop bands.

Low-temperature photoluminescence spectrum of the as-grown heterostructure reveals a peak at 702 nm (Fig. 1), which originates from the MQW regions and confirms the high quality of the sample. Surface normal (z direction)

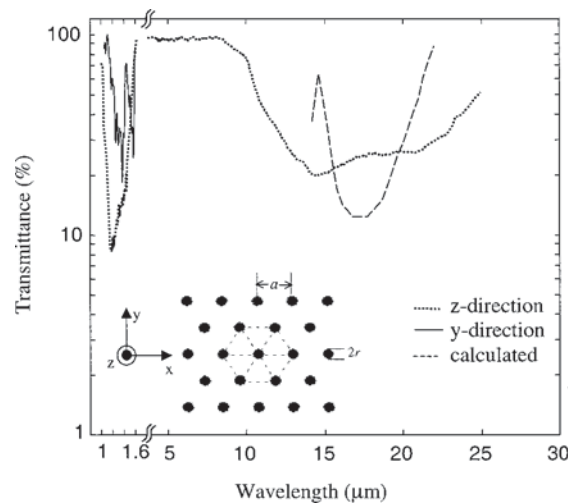


FIG. 3. Transmission spectra show a stop band between 15 and 20 μm along z direction for a PBG material with $a=6.3 \mu\text{m}$, $r=0.15\text{--}1.5 \mu\text{m}$, and index contrast of 2.36. Also shown are the stop bands around 1 μm measured along the y and z directions and the calculated stop band.

FTIR was performed at room temperature, in the wavelength range of 2.5–25 μm on samples in which the GaAs substrate was thinned down to 100 μm and polished. Since the beam size ($\sim 5 \text{ mm}$) is much larger than the waveguide width, samples with several parallel waveguides were used and normal incidence (from the top) was employed. The measured spectrum is shown in Fig. 3. The spectrum is normalized by the measured spectra of the GaAs substrate and Al_xO_y of thicknesses identical to those in the photonic crystals. A transmittance dip between 15 and 20 μm is observed, which fits reasonably well with the results¹⁶ of a 2D crystal scaled from the microwave measurements, with the parameters of our structure, using a simple scaling factor of 1146 (the ratio of center-to-center spacing of high index scatterers). This is also shown in Fig. 3. The smaller and wider transmission dip in our measured data compared to the reference results, could be due to the scatterer size nonuniformity in our crystal. Transmission spectroscopies on both surface normal (z direction) and waveguide (y direction) were also done in the wavelength range of 0.9–1.6 μm with a photomultiplier or a Ge detector. Again, the measured data were normalized with respect to GaAs and Al_xO_y . The measured spectra are also shown in Fig. 3, with a 12 dB attenuation at 1.18 μm along the z direction. A transmission peak is also noted within the stop band in the y direction. The exact origin of the second gap at the lower wavelength is not fully understood, but its presence is confirmed with measurement in two orthogonal directions. Similar gaps have been theoretically calculated by Maystre *et al.* in photonic crystals composed of dielectric rods in air or air holes in dielectric medium¹⁷ and have been attributed to grating effects due to Wood's anomalies. These authors¹⁸ also observed the introduction of doping, or defects, in the lattice produced states in the gap, like the one observed by us. It must be remembered that we are presenting a technique which could potentially be useful for realizing semiconductor-based 3D photonic crystals. In the crystal reported here, the perfect periodicity is destroyed by process-induced nonuniformity of the scatterer size. These aspects are under investigation.

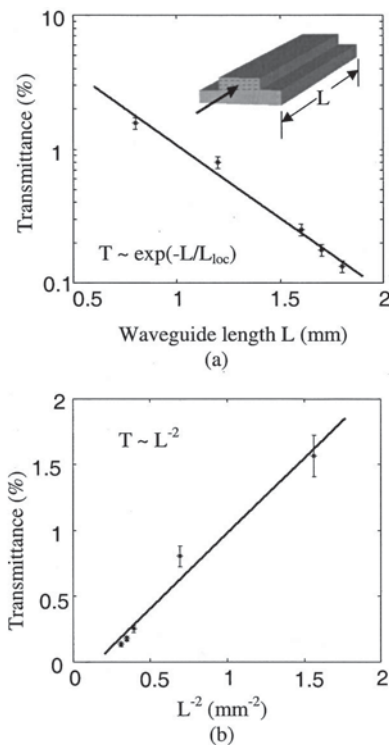


FIG. 4. Measured transmission of end-fired $1.15\ \mu\text{m}$ light through waveguides (y direction) as a function of guide length. The polarization of the incident light is parallel to the heterostructure layers. The measured transmission is fitted to: (a) exponential and (b) quadratic variation with waveguide length. Both fits are good, indicating possibly photon localization.

In order to investigate possible light localization due to the observed defect states, we have measured the transmission coefficient T as a function of waveguide length L . The GaAs substrates were completely removed in these samples in order to eliminate mode leakage into substrates. The cleaved facets of waveguides, varying in length from 0.6 to 1.8 mm, were end fired with TE polarized light from a $1.15\ \mu\text{m}$ He-Ne laser and the guided (transmitted) power at the output was measured with a power meter. We did not observe any evidence of light leaking into the thin Al_xO_y supporting layer underneath. The measured data is shown in Fig. 4(a). A distinct exponential decay of the transmission with waveguide length is observed and assuming that the decay is $\sim \exp(-L/L_{\text{loc}})$, where L_{loc} is the localization length, a value of $L_{\text{loc}} = 0.4\ \text{mm}$ is extrapolated. We have also fitted the same data with a $T \sim L^{-2}$ dependence in accordance with the scaling theory of localization at the localization transition.^{3,19,20} The fit is shown in Fig. 4(b). For a $T \sim L^{-2}$ dependence, an average transport velocity $v = 3.81 \times 10^7\ \text{cm/s}$ is estimated, assuming an average mean free path of $1.73\ \mu\text{m}$. The phase

velocity for this device, derived from a geometrical optics estimation with a fill factor of 0.26, is about $1.54 \times 10^{10}\ \text{cm/s}$. Therefore, it can be said with some caution that light localization occurs in our samples, possibly due to the localized defect states, observed in the transmission experiments.

We demonstrate here a processing technique with which we have created a quasi-3D photonic crystal. Work is in progress to improve the size uniformity and scale down the scatterer spacing by using electron-beam lithography and better controlled disordering techniques. Although it may not be immediately possible to produce symmetric fcc or diamond-like lattices, other lattice types such as simple cubic or hexagonal can be realized after eliminating the process-induced size nonuniformity.

The authors acknowledge the help provided by Professor J. Kanicki and T. Li in performing the FTIR measurements. Useful suggestions made by H. Gebretsadik and O. Qasimeh are appreciated. The work was partially supported by the Army Research Office. One of us (P.B.) gratefully acknowledges the support provided by the John Simon Guggenheim award.

¹S. John, Phys. Rev. Lett. **58**, 2486 (1987).

²E. Yablonovitch, J. Opt. Soc. Am. B **10**, 283 (1993).

³D. Wiersma, P. Bartolini, A. Lagendijk, and R. Righini, Nature (London) **390**, 671 (1997).

⁴A. Figotin and A. Klein, J. Opt. Soc. Am. A **15**, 1423 (1998).

⁵K. M. Ho, C. T. Chan, C. M. Soukoulis, R. Biswas, and M. Sigalas, Solid State Commun. **89**, 413 (1994).

⁶C. C. Chen and A. Scherer, J. Vac. Sci. Technol. B **13**, 2696 (1995).

⁷T. F. Krauss, R. M. De La Rue, and S. Brand, Nature (London) **383**, 699 (1996).

⁸S. Y. Lin, J. G. Fleming, D. L. Hetherington, B. K. Smith, R. Biswas, K. M. Ho, M. Sigalas, W. Zubrzycki, S. R. Kurtz, and J. Bur, Nature (London) **394**, 251 (1998), and references therein.

⁹S. Noda, N. Yamamoto, and A. Sasaki, Jpn. J. Appl. Phys., Part 2 **36**, L909 (1996).

¹⁰J. G. Fleming and S. Y. Lin, Opt. Lett. **24**, 49 (1999).

¹¹W. Laidig, N. Holonyak, Jr., M. D. Camras, K. Hess, J. J. Coleman, P. D. Dapkus, and J. Bardeen, Appl. Phys. Lett. **38**, 776 (1981).

¹²J. M. Dallesasse, N. Holonyak, Jr., S. R. Sugg, T. A. Richard, and N. El-Zein, Appl. Phys. Lett. **57**, 2844 (1990).

¹³J.-H. Kim, D. H. Lim, K. S. Kim, G. M. Yang, K. Y. Lim, and H. J. Lee, Appl. Phys. Lett. **69**, 3357 (1996).

¹⁴M. H. MacDougall, H. Zhao, P. D. Dapkus, M. Ziari, and W. H. Steier, Electron. Lett. **30**, 1147 (1994).

¹⁵P. W. Evans, J. J. Wierer, and N. Holonyak, Jr., Appl. Phys. Lett. **70**, 1119 (1997).

¹⁶V. Arbet-Engels, E. Yablonovitch, C. C. Cheng, and A. Scherer, in *Microcavities and Photonic Bandgaps*, edited by Rarity & Weisbuch (Kluwer Academic, The Netherlands, 1996), p. 125.

¹⁷D. Maystre, Pure Appl. Opt. **3**, 975 (1994).

¹⁸P. Sabouroux, G. Tayeb, and D. Maystre, Opt. Commun. **160**, 33 (1999).

¹⁹J. D. Joannopoulos, P. Villeneuve, and S. Fan, Nature (London) **386**, 143 (1997).

²⁰A. Z. Genack and N. Garcia, J. Opt. Soc. Am. B **10**, 408 (1993).